Catalysis Science & Technology

Accepted Manuscript

ROYAL SOCIETY OF CHEMISTRY

www.rsc.org/catalysis

Cite this: DOI: 10.1039/c0xx00000x

www.rsc.org/xxxxxx

ARTICLE TYPE

Kinetic Resolution of Phosphoric Diester by Cinchona Alkaloid Derivatives Provided with a Guanidinium Unit†

Riccardo Salvio,*[a,b] Mauro Moliterno,[a] Dario Caramelli,[a] Luca Pisciottani,[a] Achille Antenucci,[a] Melania D'Amico,[a] and Marco Bella[a]

Received (in XXX, XXX) Xth XXXXXXXXX 20XX, Accepted Xth XXXXXXXXX 20XX
DOI: 10.1039/b000000x

Cinchona alkaloid derivatives featuring a guanidinium group in diverse positions efficiently catalyze the cleavage of the RNA model compound 2-hydroxypropyl *p*-nitrophenyl phosphate (HPNP). The high catalytic efficiency as phosphodiesterases and the potentiometric and kinetic investigation indicate the existence of a high degree of cooperation between the guanidinium group and the quinuclidine moiety with the operation of a general acid/general base mechanism. The performances of these compounds were investigated and compared in the kinetic resolution of HPNP. These data were also compared with the results of DFT calculations on the transition states of the transesterification reaction that, in part, predict and rationalize the experimental data.

Introduction

The relevance of phosphodiester bonds in biology and chemistry and their reluctance towards hydrolysis[1] have encouraged many scientists to design and synthesize artificial catalysts able to cleave DNA, RNA and their model compounds,[2-4] with the idea to use these systems in health-related targets, such as the antisense therapy.[4a,5]

Most of bifunctional small-molecule enzyme-mimics contain metal cations as catalytically active groups, typically Cu^{II} an Zn^{II}.[2,3] In addition or alternatively to metal ions several artificial catalysts feature other functions as active components. These moieties play the role of anchoring sites, activators and general bases. Among these components the guanidinium group has a noteworthy importance because it has been successfully employed in the design of enzyme mimics.[2b,4] This group can interact, due to its planar and rigid structure and to its geometrical complementarity, with the phosphate anion through the formation of a two-point hydrogen bonding chelate motif.[6] In nature this guanidinium-oxanion interaction is frequently observed in enzymes and antibodies.[2b,7]

In artificial phosphodiesterases, like in all supramolecular catalysts, a primary role is played by the molecular scaffold that must be a compromise between preorganization and flexibility, keeping the active functions at the proper distance and in a favourable orientation. Diverse non chiral spacers have been used in the design of these artificial catalysts such as terpyridine,[4i] 2,2'-dipyridyl,[4j] the xylylene unit,[4c,4h,4g] calix[4]arene[8] and diphenylmethane[4b] derivatives. Another promising and emerging strategy in the preparation of artificial phosphodiesterases is the use of nanostructured supports, i.e. gold monolayer protected clusters [2a,9] (Au MPC) and polymer brushes,[10] as spacers for the active units.

In the present study we designed and developed guanidinium-based artificial phosphodiesterases derived from quinine, one of the naturally occurring Cinchona alkaloids. These compounds have attracted exceptional attention in the field of asymmetric catalysis[11] because of their ability to efficiently mediate a number of asymmetric reactions together with their commercial availability as enantiopure compounds. In their underivatized form, they can act as chiral Brønsted bases due to their quinuclidine moiety. They can be easily modified in order to improve the catalytic efficiency in enantioselective synthesis. In particular, the most common derivatives are: amino derivatives[12] capable to activate carbonyl compounds via enamine or iminium ion formation, quaternary ammonium salts acting as phase-transfer catalysts[13] and bifunctional catalysts equipped with an additional H-bond donor moiety.[14]

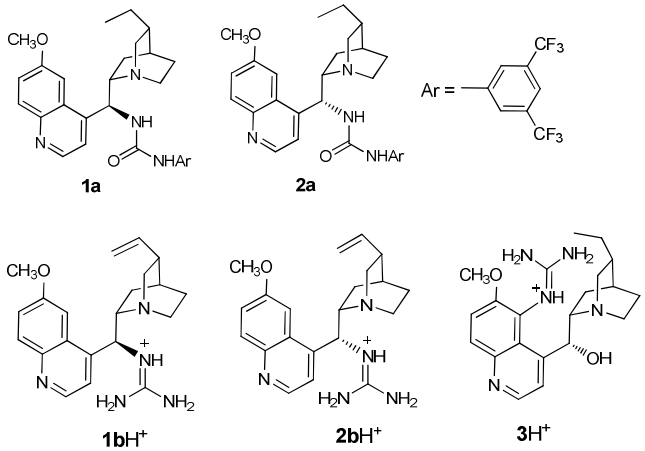

In the present study we have synthesized and investigated compounds **1b, 2b** and **3**, featuring a guanidinium unit and a tertiary amine in different relative positions and orientations on a cinchona alkaloid scaffold, as catalysts in the transesterification of the RNA model compound 2-hydroxypropyl *p*-nitrophenyl phosphate (HPNP, eq 1).

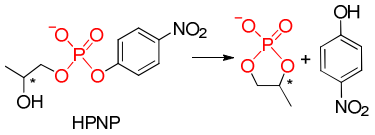

(1)

Compounds **1b** and **2b** differ in the configuration at C9, which can be crucial for the catalyst performance as observed by Connon *et al.* with the urea-substituted Cinchona alkaloid derivatives **1a** and **2a** which exhibit dramatically different yields and enantioselectivity as bifunctional catalysts in the addition of malonate to nitroalkenes.[15]

Potentiometric and kinetic evidences are presented to evaluate the catalytic efficiency and propose a catalytic mechanism. The different performances of the three catalysts are also compared in the kinetic resolution of HPNP. DFT calculations on the transition states of the transesterification reaction complement kinetic investigation providing a useful rationalization of the experimental results. In the paper we have highlighted the importance and the uniqueness of using a chiral spacer such as quinine derivatives for the synthesis of artificial phosphodiesterases, considering the fact that DNA and RNA are chiral molecules.

Results and Discussion

Synthesis of the Catalysts. The guanidine derivative **1b** was synthesized starting from 9-amino(9-deoxy)*epi* quinine (**4**)[14a] using *N*,*N*'-di Boc-thiourea and $HgCl_2$,[16] followed by the removal of protecting groups to afford the product as trihydrochloride **1b**·3HCl, (Scheme 1).

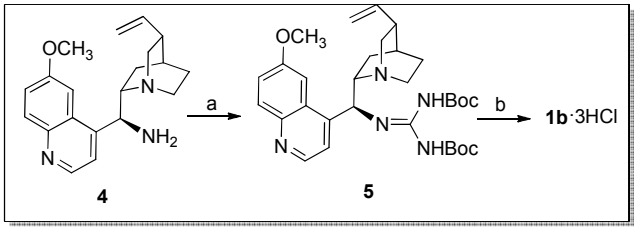

Scheme 1 Synthesis of quinine derivative **1b** starting from 9-amino(9-deoxy)*epi* quinine **4**. Reagents and conditions: a) BocNHC(S)NHBoc, $HgCl_2$, Et_3N, DMF, 12 h, rt, yield: 53% ; (b) 0.1 M HCl, 1,4-dioxane, 12 h, rt, yield: 97%.

The preparation of compound **2b** was carried out starting from the 9-*epi*quinine **6**[17] through steps *a-e* illustrated in Scheme 2. Direct synthesis of compound **9** from 9-*epi*quinine through Mitsunobu reaction afforded the desired compound in low yield. For this reason the synthesis was carried out converting the alcohol **6** into its mesylate, followed by substitution with NaN_3 and reduction with PPh_3 (steps *a-c*, Scheme 2). The guanidinylation on the 5' position affording compound **3** was carried out starting from the dihydroquinine derivative **10**[18] with the same guanidinylation method used for the synthesis of **1b** and **2b**.

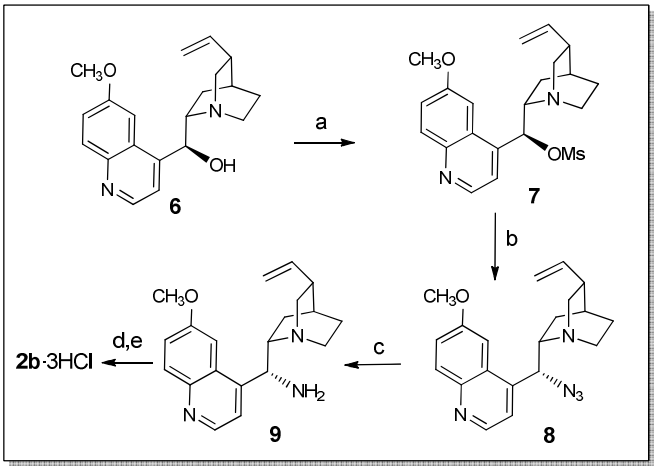

Scheme 2 Synthesis of catalyst **2b** starting from epiquinine **6**. Reagents and conditions: *a*) MsCl, Et_3N, THF, 3.5 h, rt, yield: 40%; *b*) NaN_3, DMF, 80 °C, 3 h, yield: 69%; *c*) PPh_3 in H_2O/THF 80 °C, 3 h, yield 48% *d,e*) as in steps *a* and *b* in Scheme 1, yields: 86% and 73%.

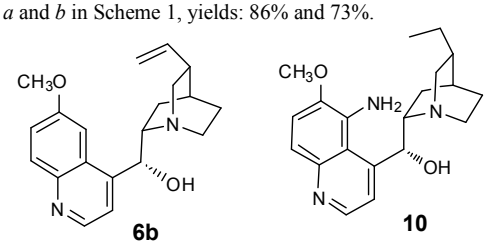

Potentiometric Titrations. The acidity constants determination of the investigated compounds is a prerequisite for the kinetic study of their catalytic properties. The potentiometric titrations were carried out in 80:20 DMSO:H_2O v/v, hereafter referred to as 80% DMSO. In this polar and protic solvent mixture, which is known to be suitable for the investigation of phosphoryl transfer reactions[4b,8,19] and for potentiometric measurements,[20] the autoprotolysis of water is strongly suppressed, $pK_w = 18.4$ at 25 °C,[21] and this implies that a neutral solution corresponds to pH 9.2. The results of the elaboration of the titration plots in Figure 1 are summarized in Table 1, together with the acidity constants of aminoquinines **4** and **9**, and the underivatized quinine (**6b**) reported for comparison.

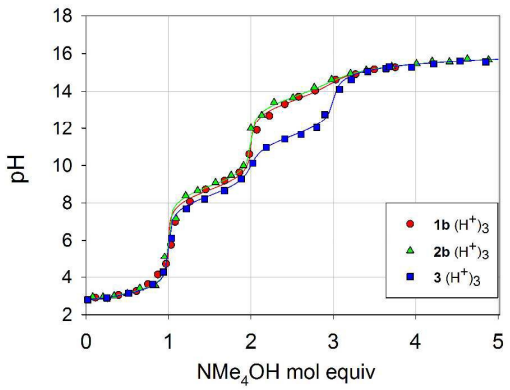

Figure 1 Potentiometric titrations of trihydrochlorides of **1b**, **2b** and **3** (2 mM) with Me_4NOH in 80% DMSO at 25 °C in the presence of 10 mM of NMe_4ClO_4. Data points are experimental and the lines are calculated.

Titrations showed three titratable protons for all the investigated compounds, except for **6b** that features only two acidic groups. **1b** and **2b** show a very similar potentiometric behavior, whereas the curve of the trihydrochloride of **3** significantly differs from the other two at higher pH values. The most acidic proton ($pK_1 < 2$) can be attributed to nitrogen atom of the quinoline unit. Acidity constants in that range cannot be accurately determined for titration carried out at millimolar concentration. This high acidity compared to quinolinium ion (pK_a=4.90)[22] is probably due to the marked electrostatic repulsion between the positively charged units, which facilitates the departure of a proton from the quinoline moiety. pK_2 is similar for compounds **1b**, **2b** and **3**, ranging from 8.4 to 8.7, and can be attributed to the quinuclidine moiety.

Table 1. Acidity Constants of Cinchona alkaloid derivatives in 80% DMSO, 25 °C.[a]

Entry	species	pK_1	pK_2	pK_3
1	**1b**$(H^+)_3$	< 2	8.7	13.5
2	**2b**$(H^+)_3$	< 2	8.9	13.7
3	**3**$(H^+)_3$	< 2	8.4	11.6
4	**4**$(H^+)_3$	2.1[b]	7.9	9.0
5	**9**$(H^+)_3$	2.2[b]	8.0	8.9
6	**6b**$(H^+)_2$	3.5	8.6	-

[a]pK_i data measured from potentiometric titrations plots in Figure 1 and in Figures 4S-6S (ESI). The titrations were carried out on 6 mL of 2 mM substrate solutions in the presence of NMe_4ClO_4. Experimental error = ± 0.1 p*K* units unless otherwise stated. [b]Experimental error = ± 0.3 p*K* units.

The least acidic protons (pK_3) in entries 1-3 belong to the guanidinium unit. The curve relative to quinine derivative **3**$(H^+)_3$ reveals a significantly higher acidity constant (pK_3, entry 3, Table 1) compared to the other two guanidine-substituted compounds (**1b** and **2b**) due to the higher acidity of aromatic guanidiniums compared to aliphatic ones.[4g,8,19] Aminoderivatives **4** and **9** show similar acidity constants (entries 4 and 5, Table 1). The least acidic proton (pK_3) can be attributed, in this case, to the quinoline unit. Consequently pK_2 is the constant associated with the deprotonation of the primary amine that is expected to be less basic than a tertiary amine. As comparison also the dihydrochloride of quinine was titrated in this set of experiments showing only two titratable protons with the acidity constants pK_1 and pK_2 indicated in entry 6 of Table 1.

Kinetic Measurements. The catalytic activity of **1b**, **2b** and **3** in the transesterification of the RNA model compound HPNP (eq 1) was investigated in the same solvent mixture and conditions used for the titrations (80% DMSO, 10 mM Me_4ClO_4, 25.0 °C).

A first set of kinetic experiments were carried out to evaluate the best pH value to carry out the measurements. Partial neutralization of 5.0 mM solutions of **1b**·3HCl with amounts of Me_4NOH afforded a number of buffer solutions with pH values in the range of around 8−12, which were used for catalytic rate measurements of HPNP transesterification using the initial-rate method. Pseudo-first-order rate constants (k_{obs}) for the cleavage of HPNP, corrected for background contributions[8] whenever appropriate (pH > 11), are reported in Figure 2. The pH−rate profile shows a maximum of activity around pH 10-12. If we assume that **1b**H^+, the monoprotonated form of the catalyst, is the only catalytically active species (eq 2), k_{obs} can be given by eq 3, where K_2 and K_3 are the acidity constants as defined in Table 1 and C_{cat} is the total catalyst concentration.

$$v = k_{cat}[\mathbf{1b}H^+][HPNP] = k_{obs}[HPNP] \qquad (2)$$

$$k_{obs} = \frac{k_{cat}C_{cat}}{\frac{K_w}{[H^+]} + 1} \qquad (3)$$

The data in Figure 2 can be fitted to a good precision to eq 3. The acidity constants (K_2, K_3) and k_{cat} were treated as adjustable parameters in a nonlinear least-square fitting procedure. The following values of best fit parameters were obtained: pK_2=8.45±0.12, pK_3= 13.58 ± 0.13, and k_{cat}= (9.2± 0.4)×10^{-3} M^{-1} s^{-1}.

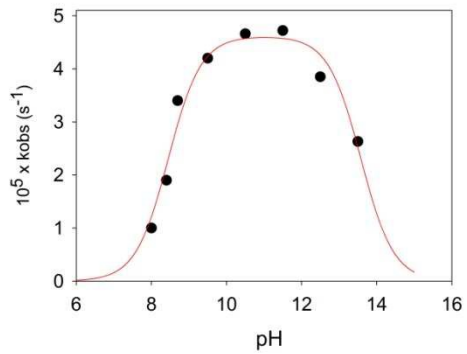

Figure 2 k_{obs} versus pH for the cleavage of 0.10 mM HPNP catalyzed by 5.0 mM **1b** in 80% DMSO, 25.0 °C, 10 mM Me_4NClO_4. The rate constants measured at pH > 11 were corrected for background hydrolysis at the given pH.

The nice fit of data points to eq 3 and the good agreement of the kinetically determined acidity constant values with the potentiometrically determined ones (pK_2 and pK_3 of entry in Table 1) are clearly consistent with the idea that **1b**H^+ is the sole active species and indicate the operation of a bifuntional mechanism in which the guanidinium is acting as an electrophilic activator and the quinuclidine moiety is acting as a general base (Figure 3).

Table 2 Transesterification of HPNP catalyzed by the listed catalysts (80% DMSO, 25 °C).[a]

entry	precatalyst	pH	$10^6\times k_{obs}$(S) (s^{-1}) [b]	$10^6\times k_{obs}$(R) (s^{-1}) [d]	k_{obs}(S)/k_{obs}(R)	$10^6\times k_{obs}$ (s^{-1}) [d]	$10^{10}\times k_{bg}$ (s^{-1}) [e]	k_{obs}/k_{bg}
1	**1b**$(H^+)_3$	8.7	62	11.6	5.2	34	32	10600
2	**2b**$(H^+)_3$	8.9	18.3	6.0	3.0	12	50	2400
3	**3**$(H^+)_3$	8.4	13.5	3.9	2.4	8.7	16	5400
4	**4**$(H^+)_3$	7.9	-[c]	-[c]	-	0.08	5.0	160
5	**9**$(H^+)_3$	8.0	-[c]	-[c]	-	0.12	6.3	190
6	**6b**$(H^+)_2$	8.6	-[c]	-[c]	-	0.10	25	40

[a] 5 mM, $[HPNP]_i$=0.1 mM, 10 mM NMe_4ClO_4; [b] determined by UV-Vis measurements with full time-course method by fitting to eq 4 and confirmed by HPLC separation with chiral column (see ref 23, Experimental Section and ESI for details), error limit=±12%. [c] too slow to be measured with the full time-course method. [d] Pseudo-first-order specific rates k_{obs} measured with the initial rate method and calculated as v_o/[HPNP], where v_o is the spectrophotometrically determined rate of *p*-nitrophenol liberation. error limit =±5% unless otherwise stated. [e] the spontaneous transesterification rate at the given pH is calculated by the following equation: $k_{bg} = 10^{(pH-17.2)}$, see ref 8.

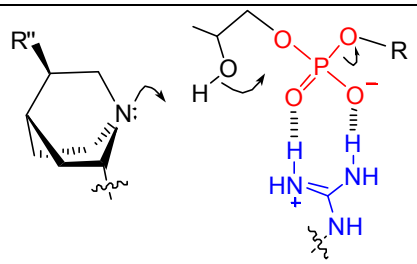

Figure 3. Proposed bifunctional mechanism for the cleavage of RNA models catalyzed by guanidine-substituted quinine derivatives involving the synergic action of a general base and an electrophilic activator.

In a second set of kinetic experiments a number of buffered solutions (pH=8.7) of catalyst **1b** at different concentrations were used for the transesterification of HPNP. The results of the kinetic experiments are graphically shown in Figure 7S (pag. 13S, ESI) as plots of pseudo-first-order rate constants (k_{obs}, s^{-1}) of HPNP cleavage versus total catalyst concentration (C_{cat}). Data points could be fitted to a straight line with the following value of best fit parameter: $k_2=(7.6\pm0.5)\times10^{-3}$ s^{-1} M^{-1}. This finding indicates that the catalyst do not significantly binds to the substrate in the investigated concentration range. This evidence is in agreement with the fact that the guanidinium-phosphate interaction has a weak binding constant in water and water/DMSO mixtures ($K < 20$ M^{-1}).[2b,19] Furthermore the straight line resulted from the fitting procedure shows an intercept close to zero, confirming that the contribution of background hydrolysis to the overall rate is negligible.

The phosphodiesterase activity of the other two catalysts (**2b** and **3**) was also investigated and the results of the kinetic experiments are reported in Table 2 together with the results obtained in the presence of the catalysts lacking of the guanidinium unit (**4**,**9** and **6b**) that were tested as control experiments. Solutions of trihydrochloride precatalysts were partially neutralized with 1.5 molar equivalents of Me_4NOH. In the resulting buffer solutions the predominant species are the di- and monoprotonated forms of the catalysts (see distribution diagrams calculated using the acidity constants in Table 1, Fig. 1-3S, ESI). These buffer solutions were used for the transesterification of HPNP with the initial rate method.

HPNP transesterification in the presence of 5.0 mM catalysts were in all cases much faster than background transesterification (k_{bg}). The rate enhancements (k_{obs}/k_{bg}) cluster around $5\cdot10^3$-fold and reach four order of magnitude in the case of guanidine-derivative **1b** (entries 1-3 of Table 2). The three catalysts exhibit also a different catalytic activity towards the two enantiomers of HPNP. For the general case in which the pseudo-first-order rate constants of the two HPNP enantiomers, k_{obs}^R and k_{obs}^S, are different the integrated kinetic equation for the formation of *p*-nitrophenol is given by (4).[23] For the particular case in which there is no kinetic resolution ($k_{obs}^R = k_{obs}^S = k_{obs}$) the concentration of *p*-nitrophenol is given by the well-known simpler equation (5).

$$[pNPhOH] = [HPNP]_o\left(1 - \frac{e^{-k_{obs}^R t} + e^{-k_{obs}^S t}}{2}\right) \quad (4)$$

$$[pNPhOH] = [HPNP]_o\left(1 - e^{-k_{obs}t}\right) \quad (5)$$

The full time-course profile of the HPNP transesterification in the presence of catalyst **1b** significantly deviate from the ordinary first-order behavior of eq 5 (see Fig 8S, ESI), but it can be fitted to good precision to eq 4. The values of k_{obs}^R and k_{obs}^S were treated in the fitting procedure as adjustable parameters obtaining the values reported in Table 2. The data about the kinetic resolution were confirmed by chiral HPLC chromatography of reaction mixtures quenched with acidic solutions at proper time intervals (see Experimental Section and ESI).

The compounds which are not provided with the guanidinium unit exhibit a dramatically lower activity in the HPNP transesterification (entries 4-6 of Table 2). These experimental evidences prove that the presence of the guanidinium unit is a key requisite to obtain high catalytic efficiency and confirm the postulated mechanism depicted in Figure 3. On the basis of kinetic data reported by Yatsimirsky et al. on the cleavage of HPNP catalyzed by amines and guanidine derivatives[19] it was possible to evaluate the effectiveness of the investigated catalytic scaffold in terms of effective molarity (EM). The EM values for compounds **1b**, **2b** and **3** are estimated to be in the range 1 – 5 M.

Ab Initio Calculations. The mechanism proposed on the basis of the kinetic measurements and schematically depicted in Figure 3 was also quantitatively investigated by *in silico* experiments. DFT calculations were carried out with Gaussian 09 package[24] at the b3lyp/6-31g(d,p)//b3lyp/6-31g(d,p) level of theory. The Berny optimization using the GEDIIS algorithm was used for the optimization procedure of the transition states of the HPNP transesterification catalyzed by catalyst **1b**H$^+$, **2b**H$^+$ and **3**H$^+$ (see Experimental Section and ESI for further details and for the coordinates of all the optimized structures). The Polarized Continuum Model was used to take into account the solvent effect, setting a dielectric constant value of 72, that is the experimental value measured in bulk for DMSO:H_2O 80:20 mixture.[19] All the TS structures feature a single imaginary frequency. The animation of the normal mode of vibration with negative spring constant confirms that the saddle points obtained from the optimization procedure are actually the transition states of the HPNP transesterification. In Figure 4 it is reported as an example the TS structure of **1b**H$^+$·(*R*)-HPNP. The geometry of the guanidinium-phosphate group and the distances H_2-O_3 and H_3-O_4 (average value=1.72 Å) indicate the presence of a chelate hydrogen bonding and not only a mere electrostatic interaction. The bond between the hydrogen atom H_1 of the HPNP hydroxyl group and the oxygen atom O_1 is breaking and a new bond is forming between the hydrogen and the quinuclidine nitrogen N_1. The distances of the bonds involved in the proton transfer (O_1-H_1= 1.42 Å H_1-N_1=1.15 Å) indicate a late transition state. The distances O_1-P (2.08 Å) and O_2-P (1.86 Å), if compared with the average P-O distance of phosphodiesters,[2b] indicate the forthcoming formation of a sigma bond and the breaking of the oxygen-phosphorous bond of the leaving group. In addition, the measure of O_3-P-O_4 angle is 121,3°, therefore significantly different from the tetrahedral geometry of the phosphate group of a phosphodiester. These findings suggest the operation of an A_ND_N concerted mechanism rather than a A_N+D_N,[2a,2b] also labeled by Kirby as $S_N2(P)$,[25] consistently with the presence of a good leaving group such as the *p*-nitrophenolate.[26]

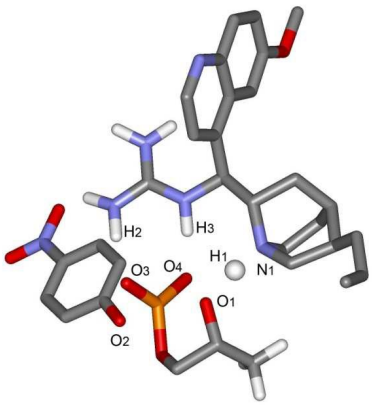

Figure 4 Transition state structure (DFT Calculations) for the transesterification of (*R*)-HPNP catalyzed by **1b**H$^+$. Some of the hydrogen atoms are omitted for clarity.

The results of the calculations on the transition states of HPNP transesterification catalyzed by the investigated compounds are reported in Table 3. The difference of the energies of the transition states for the two enantiomers is significantly higher in the presence of catalyst **1b**H$^+$. In the case of the other two catalysts the energy difference is much lower and does not reach 1 kcal/mol. On the basis of this energy difference the ratio between the observed rate constants of the two enantiomers was calculated using the Eyring equation. These values are in fair agreement with the experimental data in the last column of Table 2. (*S*)-HPNP turns out to be more reactive than (*R*) enantiomer in all cases. This is probably due to the repulsive interaction of the (*R*)-HPNP methyl group with the bulky quinine scaffold, specifically with the quinuclidine moiety (see Figure 4). The largest energy difference is predicted in the presence of **1b**H$^+$, as observed in the kinetic measurements, even though a larger rate constant ratio is calculated for a difference of 2.1 kcal/mol.

Table 3 Difference in the transition state energies (DFT calculations) for the transesterification of the two HPNP enantiomers catalyzed by the listed species and corresponding calculated ratio of the rate constants of the reactions.

Catalyst	$\Delta E^{\neq}$ ($E^{\neq}_R$- $E^{\neq}_S$) [a] (kcal/mol)	k_{obs}(S)/k_{obs}(R) cld[b]
1bH$^+$	2.11	36
2bH$^+$	0.13	1.2
3H$^+$	0.81	3.9

[a] Difference between the energies of the transition states corrected for the zero-point vibrational energy determined by frequency calculation; DFT b3lyp/6 31g(d,p)//b3lyp/6 31g(d,p), PCM, ε=72.0; See ESI and Experimental Section for further details and for the coordinates of all the optimized structurs. [b] Ratio of the transesterification rate constants k_{obs}(S) and k_{obs}(R), calculated with the Eyring equation, on the basis of the energy differences obtained by *ab initio* calculations.

Conclusions

Here we have presented the design, the synthesis and the investigation on the catalytic activity of quinine-derived guanidines as phosphodiesterases. These compounds feature a guanidinium unit in diverse position on the molecular scaffold. Potentiometric and kinetic investigation at different pH and at different catalyst concentrations demonstrate the operation of a general-acid/general-base mechanism (Figures 3 and 4). Species **1b**H$^+$, **2b**H$^+$ and **3**H$^+$ turn out to be very effective catalysts of HPNP transesterification with rate enhancements relative to the background hydrolysis approaching four orders of magnitude in case of **1b**H$^+$. These data suggest that the configuration of C9 plays a crucial role in modulating the activity of the catalysts. Interestingly the same compound is slightly stereoselective in the kinetic resolution of HPNP. This experimental evidences are supported by DFT calculations on the transition states of transesterification which confirm the postulated mechanism. The calculations show geometrical complementarity between the catalysts and the substrate and quantitatively predict, with fairly

good agreement with experimental data, the ratio between the observed rate constant of the transesterification reaction. These results provide a useful comparison between experimental and *in silico* data which are potentially useful in the design of artificial ribonucleases, and, in general, in catalysis by design.

Experimental Section

Instruments and general methods

^{1}H and ^{13}C NMR spectra were recorded on a Bruker 300 MHz spectrometer. Chemical shifts are reported as δ values in ppm. In some cases small amount of TMS or dioxane were used as an internal standard. High-resolution Mass-spectrometric analysis was performed by on an electrospray ionization time-of-flight spectrometer. Ab initio calculation were carried out with Gaussian 09 (Revision D.01) package[24] using Narten Cluster – Dipartimento di Chimica - Sapienza. Chiral HPLC separation was performed employing a CHIRALPAK IA column.

Materials

HPNP,[27] 9-amino(9-deoxy)*epi* quinine (**4**)[14a], 9-*epi* quinine (**6**),[17] and 5'-aminodihydro quinine (**10**)[18] were prepared as reported in the literature. DMSO was purged for 30 min with argon to eliminate volatile sulphide impurities and mQ water was used in the preparation of 80:20 DMSO:H_2O v/v. Anhydrous dichloromethane was obtained by distillation over $CaCl_2$. Triethylamine was distilled over KOH. Anhydrous THF was obtained by distillation over Na. Other reagents and solvents were commercially available and used without any further purification.

9-Bis[4-(N,N-di(tert-butoxycarbonyl)guanidine(9-deoxy)*epi* quinine (5) 507 mg of 9-amino(9-deoxy)*epi* quinine (**4**, 1.57 mmol), *N*,*N*'-Di-Boc-thiourea (362 mg, 1.31 mmol) and 0.50 mL of triethylamine were dissolved in dry DMF under argon atmosphere. The reaction flask was cooled down to 0 °C and $HgCl_2$ (354 mg, 1.31 mmol) was added to the solution. The mixture was stirred for 12 h at room temperature. Then 10 mL of ethyl acetate were added and the HgS eliminated by filtration through a pad of celite. A pure sample of **5** was obtained by flash column chromatography (SiO_2, AcOEt/hexane 3:2) as a colorless sticky solid (395 mg, 53% yield). ^{1}H NMR (300 MHz, $CDCl_3$): δ 1.39 (s, 9H), 1.44 (s, 9H), 1.55-1.85 (m, 6H), 2.35 (bs, 1H), 2.70-3.05 (m, 2H), 3.21-3.59 (m, 3H), 4.0 (s, 3H), 5.04 (m, 2H), 5.81 (m, 1H), 7.33-7.42 (m. 2H), 7.83 (s, 1H), 8.03 (d, 1H, 12 Hz), 8.75 (s, 1H), 8.77 (s, 1H), 11.32 (s, 1H). ^{13}C NMR (75 MHz, $CDCl_3$): δ 26.9, 27.5, 27.8, 28.1, 28.2, 39.5, 41.3, 55.8, 56.1, 59.3, 78.5, 82.9, 102.1, 114.5, 119.7, 122.3, 128.5, 131.3, 161.6, 144.4, 144.8, 147.4, 152.8, 155.4, 157.9, 163.3. HR ES-MS: *m/z* Calcd for $C_{31}H_{44}N_5O_5$ $(M+H)^+$: 566.3342, found 566.3336.

9-Guanidine(9-deoxy)*epi* quinine tris-hydrochloride (1b·3HCl) A solution of compound **5** (136 mg, 0.240 mmol) in 20 mL of a 1:1 v/v mixture of dioxane and 0.5 M hydrochloric acid was stirred for 12 hours at room temperature. Evaporation of the solvent gave compound **1**·3HCl as a white sticky solid (111 mg, 0.234 mmol, 97% yield). ^{1}H NMR (300 MHz, D_2O): δ 1.26-1.44 (m, 1H), 1.63-1.77 (tr, 1H, J=12 Hz), 1.97-2.20 (m, 3H), 2.81-2.96 (m, 2H), 3.41-3.56 (m, 2H), 3.67-3.80 (tr, 1H, J=14 Hz), 3.90-4.02 (m, 1H), 4.08 (s, 3H), 4.13-4.25 (m, 1H), 5.08-5.25 (m, 2H), 5.70-5.88 (m, 1H), 7.79-7.93 (m, 2H), 8.12-8.28 (m, 2H), 9.00 (d, 1H, 6 Hz). ^{13}C NMR (75 MHz, D_2O): δ 23.4, 24.0, 26.1, 30.2, 36.3, 43.0, 54.1, 57.5, 60.7, 103.4, 117.3, 121.7, 124.0, 128.6, 130.1, 134.7, 137.8, 141.4, 150.9, 157.3, 161.8. HR ES-MS: *m/z* Calcd for $C_{21}H_{28}N_5O$ $(M+H)^+$ 366.2294, found 366.2289.

9-Methanesulfonate(9-deoxy)*epi* quinine (7) 2.71 g of **6** (8.35 mmol) and 4.6 ml of triethylamine were dissolved in dry THF under nitrogen atmosphere. The reaction flask was cooled down to 0 °C and mesyl chloride (1.33 ml, 17.2 mmol) was added dropwise to the solution. The mixture was stirred for 30 minutes at 0°C then 3.5 hours at room temperature. After that the solvent was evaporated under reduced pressure. The residue was dissolved in dichloromethane (400 mL) and washed with a 3.5% $NaHCO_3$ aqueous solution (3 x 200 mL). The organic phase was dried over Na_2SO_4 and evaporated. The crude material was purified by column chromatography (SiO_2; CH_2Cl_2/MeOH 14:1) giving a pale yellow amorphous solid (1.351 g, 3.36 mmol, 40% yield). ^{1}H NMR (300 MHz, $CDCl_3$): δ 0.63-0.75 (m, 1H), 1.27-1.48 (m, 1H), 1.49-1.58 (m, 2H), 1.60-1.67 (m, 1H), 2.20-2.32 (bs, 1H), 2.72-2.85 (m, 2H), 2.88-3.07 (bs, 3H), 3.15-3.28 (m, 1H), 3.25-3.50 (br, 2H), 3.94 (s, 3H), 4.90-5.05 (m, 2H), 5.62-5.87 (m, 1H), 6.30 (bs, 1H), 7.37 (d, 1H, J=3 Hz), 7.40 (d, 1H, J=3 Hz), 7.46 (m, 1H), 8.03 (d, 1H, 9 Hz), 8.76 (s, 1H). ^{13}C NMR (75 MHz, $CDCl_3$): δ 24.9, 27.2, 27.6, 39.0, 39.2, 41.0, 55.5, 59.6, 76.6, 100.4, 114.5, 119.6, 122.1, 127.2, 131.9, 139.6, 141.2, 144.8, 147.3, 158.3. HR ES-MS: *m/z* Calcd for $C_{21}H_{27}N_2O_4S$ $(M+H)^+$: 403.1692, found 403.1685.

9-Azido(9-deoxy) quinine (8) 1.35 g of 9-methanesulfonate(9-deoxy)*epi* quinine (**7**, 3.36 mmol) were dissolved in DMF under nitrogen atmosphere. Sodium azide (0.813 g, 12.5 mmol) was added to the solution. The mixture was stirred for 3 hours at 80°C and then one night at room temperature. After that the mixture was evaporated under reduced pressure. 400 mL of a 1M NaOH aqueous solution and dichloromethane (400 mL) were added to the residue. The organic phase was separated, washed with a 1M NaOH aqueous solution (3x200 mL), and dried over Na_2SO_4. The solvent was evaporated and the crude material was purified by column chromatography (SiO_2; CH_2Cl_2/MeOH 100:1). Compound **8** was obtained ad white amorphous solid (0.813 g, 2.33 mmol, 69% yield). ^{1}H NMR (300 MHz, $CDCl_3$): δ 1.45-1.80 (m, 3H), 1.80-1.99 (m, 2H), 2.23-2.37 (m, 1H), 2.57-2.75 (m, 2H), 3.01-3.35 (m, 3H), 3.97 (s, 3H), 4.96-5.05 (m, 2H), 5.17-5.37 (bs, 1H), 5.70-5.89 (m, 1H), 7.30-7.36 (m, 1H), 7.36-7.43 (m, 2H), 8.06 (d, 1H, J=9 Hz), 8.79 (d, 1H, J=3 Hz). ^{13}C NMR (75 MHz, $CDCl_3$): δ 24.7, 27.2, 27.5, 39.4, 42.1, 55.8, 56.5, 58.4, 65.0, 101.0, 114.7, 119.5, 121.8, 127.0, 132.0, 141.3, 141.7, 144.9, 147.5, 158.2. HR ES-MS: *m/z* Calcd for $C_{20}H_{24}N_5O$ $(M+H)^+$:350.1981, found 350.1992.

9-amino(9-deoxy) quinine (9) 2.46 g of 9-azido(9-deoxy)*epi* quinine (**8**, 7.04 mmol) and triphenylphosphine (4.14 mg, 15.8 mmol) were dissolved in dry THF under nitrogen atmosphere. The mixture was stirred for 3 hours at 80°C. After cooling 1 mL of water was added and the reaction mixture was stirred for 12 h at room temperature. Afterward the solvent was evaporated under

reduced pressure and the residue dissolved in 10% aqueous HCl (400 mL) and washed with dichloromethane (3 x 200 mL). 1M NaOH aqueous solution was added to the water phase until alkaline pH was reached. The mixture was extracted with dichloromethane and the organic phase was dried over Na_2SO_4. The crude material was purified by column chromatography (SiO_2, CH_2Cl_2/MeOH 30:1). Compound **9** was obtained as a pale yellow oil (1.10 g, 3.41 mmol; 48% yield). ^{1}H NMR (300 MHz, $CDCl_3$): δ 1.45-1.63 (m, 2H), 1.64-1.78 (m, 2H), 1.83-1.95 (m, 2H), 2.08-2.21 (m, 1H), 2.24-2.35 (m, 1H), 2.47-2.75 (m, 2H), 2.95-3.12 (m, 2H), 3.13-3.26 (m, 1H), 3.96 (s, 3H), 4.65 (d, 1H, J=9 Hz), 5.00-5.13 (m, 2H), 5.84-6.00 (m, 1H), 7.32-7.39 (m, 2H), 7.43 (d, 1H, J=3 Hz), 8.02 (d, 1H, J=12 Hz), 8.73 (d, 1H, J=3 Hz). ^{13}C NMR (75 MHz, $CDCl_3$): δ 26.3, 27.7, 39.6, 41.9, 53.6, 55.6, 56.1, 60.5, 101.1, 114.4, 118.2, 121.1, 127.6, 131.9, 141.7, 144.7, 147.8, 149.1, 157.7. HR ES-MS: *m/z* Calcd for $C_{20}H_{26}N_3O$ $(M+H)^+$: 324.2076, found 324.2089.

9-Bis[4-(N,N-di(tert-butoxycarbonyl)guanidine(9-deoxy) quinine (9b) 600 mg of 9-amino(9-deoxy) quinine (**9**, 1.86 mmol), *N*,*N*'-Di-Boc-thiourea (513 mg, 1.86 mmol) and 0.8 mL of triethylamine were dissolved in dry DMF under nitrogen atmosphere. The reaction flask was cooled down to 0 °C and $HgCl_2$ (1.25 g, 4.62 mmol) was added portionwise. The mixture was stirred for one night at room temperature and then 50 mL of ethyl acetate were added and the HgS precipitate was eliminated by filtration through celite. After solvent removal at reduced pressure a pure sample of **9b** was obtained by flash column chromatography (SiO_2, CH_2Cl_2/MeOH/Et_3N 100:0.5:0.25) as a colorless white solid (904 mg, 86% yield): mp 150-152 °C. ^{1}H NMR (300 MHz, $CDCl_3$): δ 1.10-1.30 (m, 1H), 1.45 (s, 9H), 1.47 (s, 9H), 1.65-2.05 (m, 3H), 2.21-2.41 (m, 1H), 2.55-2.88 (m, 3H), 2.90-3.15 (m, 2H), 3.40-3.58 (m, 1H), 3.99 (s, 3H), 4.98-5.14 (m, 2H), 5.81-6.05 (m, 1H), 6.21-6.35 (m, 1H), 7.32-7.43 (m, 2H), 7.81 (s, 1H), 8.98 (d, 1H, J=9 Hz), 8.71 (bs, 1H), 8.75 (d, 1H, J=6 Hz), 11.43 (bs, 1H). ^{13}C NMR (75 MHz, $CDCl_3$): δ25.1, 27.6, 28.0, 28.2, 39.5, 42.1, 46.1, 51.0, 56.1, 56.4, 58.3, 79.3, 83.7, 101.8, 114.6, 118.8, 122.4, 128.1, 131.5, 141.6, 144.3, 145.0, 147.5, 153.1, 156.3, 158.1, 163.3. HR ES-MS: *m/z* Calcd for $C_{31}H_{44}N_5O_5$ $(M+H)^+$: 566.3342, found 566.3329.

9-Guanidine(9-deoxy) quinine tris-hydrochloride (2b·3HCl) A solution of compound **9b** (100 mg, 0.18 mmol) in 0,41 mL of TFA and 1 mL of dichloromethane was stirred for 2 hours at room temperature. The solution was evaporated, dried under vacuum, and the solid dissolved in 10 mL of 1 M HCl. Evaporation of the solvent gave the compound as a sticky white solid (142 mg, 0.142 mmol, 73% yield). ^{1}H NMR (300 MHz, D_2O): δ 1.91-2.49 (m, 4H), 2.65-2.75 (m, 1H), 2.80-2.98 (m, 1H), 3.05-3.55 (m, 3H), 3.58-3.78 (m, 1H), 4.11 (s, 3H), 4.28-4.48 (m, 1H), 5.15-5.38 (m, 2H), 5.85-5.95 (m, 1H), 5.95-6.10 (m, 1H), 7.83 (d, 1H, J=12 Hz), 7.90-8.00 (m, 1H), 8.15-8.35 (m, 2H), 9.00-9.15 (m, 1H). ^{13}C NMR (75 MHz, D_2O): δ 23.7, 24.3, 25.9, 36.3, 43.5, 54.8, 57.4, 60.3, 63.1, 67.2, 102.3, 117.8, 121.5, 124.9, 128.7. HR ES-MS: *m/z* Calcd for $C_{21}H_{28}N_5O$ $(M+H)^+$: 366.2294, found 366.2286

5'-[(N,N-di(tert-butoxycarbonyl)guanidine dihydroquinine (11) 252 mg of compound **10** (0.74 mmol), *N*,*N*'-Di-Boc-thiourea (328 mg, 1.19 mmol) and 0.30 mL of triethylamine were dissolved in dry DMF under nitrogen atmosphere. The reaction flask was cooled down to 0 °C and $HgCl_2$ (525 mg, 1.93 mmol) was added to the solution. The mixture was stirred for 24 h at room temperature and then 10 mL of ethyl acetate were added and the precipitated HgS eliminated with filtration through celite. A pure sample of **11** was obtained by flash column chromatography (SiO_2, AcOEt/MeOH 100:1) as a yellow sticky solid (151 mg, 0.26 mmol, 35% yield). ^{1}H NMR (300 MHz, $CDCl_3$): δ 0.87 (tr, 3H, J=6 Hz), 1.34-1.48 (m, 4H), 1.53 (s, 18H), 1.58-1.75 (m, 2H), 1.77-1.87 (bs, 1H), 2.05-2.21 (m, 1H), 2.41 (d, 1H, J=15 Hz), 2.57-2.72 (m, 1H), 2.91-3.13 (m, 2H), 3.47-3.67 (m, 1H), 4.08 (s, 3H), 5.49 (d, 1H, J=9 Hz), 7.39 (d, 1H, J=3Hz), 7.51 (d, 1H, J=9Hz), 7.90 (d, 1H, J=9 Hz), 8.71 (d, 1H, J= 3 Hz), 12.09 (bs, 1H). ^{13}C NMR (75 MHz, $CDCl_3$): δ 12.8, 25.4, 26.2, 28.8, 29.0, 38.1, 42.5, 57.9, 58.1, 58.5, 80.9, 82.6, 116.3, 119.5, 120.6, 121.5, 121.8, 127.0, 142.6, 144.7, 146.1, 149.2. HR ES-MS: *m/z* Calcd for $C_{31}H_{46}N_5O_6^+$ $(M+H)^+$: 584.3448, found 584.3474.

5'-Guanidine dihydroquinine Tris-hydrochloride (3·3HCl) A solution of compound **11** (26 mg, 0.044 mmol) in 4 mL of a 1:1 v/v mixture of dioxane and 0.1 M hydrochloric acid was stirred for 24 hours at room temperature. Evaporation of the solvent gave compound **3**·3HCl as a sticky white solid (16.1 mg, 0.042 mmol, 96% yield), mp 128-129 °C. ^{1}H NMR (300 MHz,): δ 0.87 (tr, 3H, J=9 Hz), 1.25-1.43 (m,1H), 1.50-1.78 (m, 3H), 1.95-2.17 (m, 3H), 2.81-2.96 (m, 1H), 3.39-3.64 (m, 3H), 3.65-3.80 (m, 1H), 3.88-4.03 (m, 1H), 4.08 (s, 3H), 5.04 (d, 1H, J=9 Hz), 7.65 (d, 1H, 9 Hz), 7.83 (d, 1H, 6 Hz), 8.42 (d, 1H, 9Hz), 8.97 (d, 1H, 6 Hz). ^{13}C NMR (75 MHz,): δ 10.8, 22.6 24.1, 26.3, 26.9, 36.1, 41.3, 55.9, 56.7, 58.2, 69.6, 114.0, 117.8, 121.2, 113.3, 133.4, 142.1, 143.9, 148.0, 148.4, 155.1, 157.1. HR ES-MS: *m/z* Calcd for $C_{21}H_{30}N_5O_2$ (MH+): 384.2394, found 384.2403.

Potentiometric Titrations

Potentiometric titrations were performed by an automatic titrator equipped with a combined with a glass pH microelectrode. Experimental details and procedure for the electrode calibration in 80% DMSO were the same as previously reported.[4b,8]

Potentiometric titrations were carried out under an argon atmosphere, on 6 mL of 2 mM solutions of the investigated compounds, in the presence of 10 mM Me_4NClO_4, (80% DMSO, 25 °C). A 50-70 mM Me_4NOH solution in 80% DMSO was automatically added to the titration vessel in small increments. Analysis of titration plots was carried out by the program HYPERQUAD 2000.[28] Distribution diagrams of the species were calculated using the acidity constants determined by potentiometric titrations.

Kinetic Measurements

Kinetic measurements of HPNP cleavage were carried out by UV−vis monitoring of *p*-nitrophenol liberation at 400 nm on a diode array spectrophotometer. Rate constants reported in Table 2 were obtained by an initial rate method or full-time course experiments, error limits on the order of ±5% unless otherwise stated. The $k_{obs}(S)/k_{obs}(R)$ ratio and the absolute configuration

were confirmed by HPLC separation of the unreacted HPNP enantiomers by quenching the reaction mixture with a solution of $HClO_4$ in 80% DMSO. The following equation was used: $k_{obs}(S)/k_{obs}(R)=\ln[(1-c)(1-ee)]/\ln[(1-c)(1+ee)]$, see ref 23 and pag 15S, ESI for further details.

Ab Initio Calculations

DFT calculations were carried out at the b3lyp/6-31g(d,p)//b3lyp/6-31G(d,p) level of theory (GAUSSIAN-09 package).[24] The Berny algorithm was used to find the transition states of the transesterification reaction (*opt=ts*). The keywords *cartesian*, *calcfc* and *noeigentest* were used in the optimization of the structure to avoid errors and accelerate the conversion to the optimized structures. All the energy values were corrected for the zeropoint vibrational energy. Vibrational analysis confirmed all stationary points to be first order saddle points (one imaginary frequency). The animation of the normal mode of vibration with negative spring constant confirmed that the saddle points resulted from the optimization procedure are actually the transition states of the HPNP transesterification. The Polarized Continuum Model was used to take into account the solvent effect. The solvent parameters were set by using the following keyword and options: *scrf*= (*pcm*, *read*). *eps*=72 was used in the separate PCM input section to define the solvent mixture dielectric constant.[19] The command *AddSphereonH=N* was used in the PCM input section to place an individual sphere on the two guanidinium hydrogen atoms involved in the interaction with the phosphate and on the hydrogen atom of the HPNP hydroxyl. Energies and coordinated of the calculations are reported in Electronic Supplementary Information.

Acknowledgements

The authors thanks Chiesa Valdese Italiana and Sapienza University –"Progetti di Ateneo 2014" for financial support. Professor Luigi Mandolini and Dr. Roberta Cacciapaglia are acknowledged for the fruitful discussions. The authors also acknowledge Prof. Ruggero Caminiti for providing computing time on NARTEN Cluster HPC Facility.

Notes and references

[a] *Dipartimento di Chimica, Università di Roma – Sapienza, Italy. Tel: +39 06 4969 3656.*

[b] *IMC-CNR Sezione Meccanismi di Reazione, Università di Roma – Sapienza*

E-mail: riccardo.salvio@uniroma1.it

† Electronic Supplementary Information (ESI) available: [^{1}H and ^{13}C spectra of compounds, distribution diagrams, titrations, kinetic experiments, energies and coordinates of DFT calculations]. See DOI: 10.1039/b000000x/

1 R. Wolfenden, *Chem. Rev.*, 2006, **106**, 3379-3396.

2 for review articles see: a) F. Mancin, P. Scrimin and P. Tecilla, *Chem. Comm.*, 2012, **48**, 5545. b) R. Salvio, *Chem. Eur. J.*, 2015, **21**, 10960; c) M. Raynal, P. Ballester, A. Vidal-Ferran and P. W. van Leeuwen, *Chem. Soc. Rev.*, 2014, **43**, 1734; d) J.-N. Rebilly, B. Colasson, O. Bistri, D. Over and O. Reinaud, *Chem. Soc. Rev.*, 2015, **44**, 467; e) R. Cacciapaglia, S. Di Stefano, L. Mandolini and R. Salvio, *Supramol. Chem.*, 2013, **25**, 537; f) H. Lönnberg, *Org. Biomol. Chem.*, 2011, **9**, 1687; g) Y. Aiba, J. Sumaoka and M. Komiyama, *Chem. Soc. Rev.*, 2011, **40**, 5657; h) T. Niittymäki and H. Lönnberg, *Org. Biomol. Chem.*, 2006, **4**, 15.

3 a) M. Diez-Castellnou, F. Mancin and P. Scrimin, *J. Am. Chem. Soc.*, 2014, **136**, 1158; b) H. Korhonen, T. Koivusalo, S. Toivola and S. Mikkola, *Org. Biomol. Chem.*, 2013, **11**, 8324; c) M. F. Mohamed and R. S. Brown, *J. Org. Chem.*, 2010, **75**, 8471; d) R. Cacciapaglia, A. Casnati, L. Mandolini, D. N. Reinhoudt, R. Salvio, A. Sartori and R. Ungaro, *J. Am. Chem. Soc.*, 2006, **128**, 12322; e) R. Cacciapaglia, A. Casnati, L. Mandolini, D. N. Reinhoudt, R. Salvio, A. Sartori and R. Ungaro, *J. Org. Chem.*, 2005, **70**, 624; f) T.-S. A. Tseng and J. N. Burstyn, *Chem. Comm.*, 2008, 6209; g) K. Nwe, C. M. Andolina and J. R. Morrow, *J. Am. Chem. Soc.*, 2008, **130**, 14861; h) R. Cacciapaglia, A. Casnati, L. Mandolini, A. Peracchi, D. N. Reinhoudt, R. Salvio, A. Sartori and R. Ungaro, *J. Am. Chem. Soc.*, 2007, **129**, 12512; i) A. Scarso, G. Zaupa, F. B. Houillon, L. J. Prins and P. Scrimin, *J. Org. Chem.*, 2007, **72**, 376; j) H. Korhonen, S. Mikkola and N. H. Williams, *Chem. Eur. J.*, 2012, **18**, 659.

4 for guanidine-based systems see: a) C. Gnaccarini, S. Peter, U. Scheffer, S. Vonhoff, S. Klussmann and M. W. Göbel, *J. Am. Chem. Soc.*, 2006, **128**, 8063. b) R. Salvio, L. Mandolini and C. Savelli, *J. Org. Chem.*, 2013, **78**, 7259. c) L. Tjioe, A. Meininger, T. Joshi, L. Spiccia and B. Graham, *Inorg. Chem.*, 2011, **50**, 4327; d) R. Salvio, S. Volpi, R. Cacciapaglia, A. Casnati, L. Mandolini and F. Sansone, *J. Org. Chem.*, 2015, **80**, 5887; e) S. Ullrich, Z. Nazir, A. Busing, U. Scheffer, D. Wirth, J. W. Bats, G. Durner and M. W. Gobel, *ChemBioChem*, 2011, **12**, 1223; f) X. Sheng, X. Lu, C. Y., G. Lu, J. Zhang, Y. Shao, F. Liu and Q. Xu, *Chem. Eur. J.*, 2007, **13**, 9703; g) R. Salvio, R. Cacciapaglia and L. Mandolini, *J. Org. Chem.*, 2011, **76**, 5438. h) U. Scheffer, A. Strick, V. Ludwig, S. Peter, E. Kalden and M. W. Göbel, *J. Am. Chem. Soc.*, 2005, **127**, 2211; i) H. Ait-Haddou, J. Sumaoka, S. L. Wiskur, J. F. Folmer-Andersen and E. V. Anslyn, *Angew. Chem. Int. Ed.*, 2002, **41**, 4014; j) J. He, P. Hu, Y. J. Wang, M. L. Tong, H. Sun, Z. W. Mao and L. N. Ji, *Dalton Trans*, 2008, 3207.

5 a) A. Demesmaeker, R. Haner, P. Martin and H. E. Moser, *Acc. Chem. Res.*, 1995, **28**, 366; b) M. E. Gleave and B. P. Monia, *Nat. Rev. Cancer*, 2005, **5**, 468.

6 D. M. Perreault, L. A. Cabell and E. V. Anslyn, *Bioorg. Med. Chem.*, 1997, **5**, 1209.

7 a) F. A. Cotton, E. E. J. Hazen and M. J. Legg, *PNAS*, 1979, **76**, 2551; b) K. A. Schug and W. Lindner, *Chem. Rev.*, 2005, **105**, 67.

8 L. Baldini, R. Cacciapaglia, A. Casnati, L. Mandolini, R. Salvio, F. Sansone and R. Ungaro, *J. Org. Chem.*, 2012, **77**, 3381.

9 a) G. Zaupa, C. Mora, R. Bonomi, L. J. Prins and P. Scrimin, *Chem. Eur. J.*, 2011, **17**, 4879; b) R. Salvio and A. Cincotti, *RSC Adv.*, 2014, **4**, 28678.

10 C. Savelli and R. Salvio, *Chem. Eur. J.*, 2015, **21**, 5856.

11 a) C. E. Song, Ed. *Cinchona Alkaloids in Synthesis and Catalysis: Ligands, Immobilization and Organocatalysis*, John Wiley & Sons, Inc., 2009 b) S. J. Connon, *Chem. Comm.*, 2008, 2499; c) R. Salvio, M. Moliterno and M. Bella, *Asian J. Org. Chem.*, 2014, **3**, 340; d) C. Palomo, M. Oiarbide and R. Lopez, *Chem. Soc. Rev.*, 2009, **38**, 632.

12 (a) T. Marcelli and H. Hiemstra, *Synthesis*, 2010, **8**, 1229; (b) C. Cassani, R. Martin-Rapun, E. Arceo, F. Bravo and P. Melchiorre, *Nat. Protoc.*, 2013, **8**, 325.

13 S. S. Jew and H. G. Park, *Chem. Comm.*, 2009, 7090.

14 (a) B. Vakulya, S. Varga, A. Csámpai and T. Soós, *Org. Lett.*, 2005, **7**, 1967; b) B.-J. Li, L. Jiang, M. Liu, Y.-C. Chen, L.-S. Ding and Y. Wu, *Synlett*, 2005, **4**, 603; c) J. Ye, D. J. Dixon and P. S. Hynes, *Chem. Comm.*, 2005, 4481; d) S. J. Connon, *Chem. Eur. J.*, 2006, **12**, 5418. For the synthesis and use of other guanidine-functionalized Cinchona alkaloids see: e) X. Han, F. Zhong and Y. Lu, *Adv. Synth. Catal.*, 2010, **352**, 2778.

15 S. H. McCooey and S. J. Connon, *Angew. Chem. Int. Ed.*, 2005, **44**, 6367.

16 Y. F. Yong, J. A. Kowalski and M. A. Lipton, *J. Org. Chem.*, 1997, **62**, 1540.

17 A. E. Taggi, A. M. Hafez, H. Wack, B. Young, D. Ferraris and T. Lectka, *J. Am. Chem. Soc.*, 2002, **124**, 6626.

18 C. Palacio and S. J. Connon, *Org. Lett.*, 2011, **13**, 1298.

19 D. O. Corona-Martinez, O. Taran and A. K. Yatsimirsky, *Org. Biomol. Chem.*, 2010, **8**, 873.

20 M. Georgieva, *Anal. Chim. Acta*, 1977, **90**, 83; b) R. Wróbel and L. Chmurzyński, *Anal. Chim. Acta*, 2000, **405**, 303.

21 M. M. Kreevoy and E. H. Baughman, *J. Phys. Chem.*, 1974, **78**, 421.

22 *CRC Handbook of Chemistry and Physics*, 90th Ed.; Lide, D.R., Ed.; CRC Press: Boca Raton, FL, 2010; Section 8-48, p 1241.
23 for a review about the quantitative treatment of kinetic resolution see: J. M. Keith, J. F. Larrow and E. N. Jacobsen, *Adv. Synth. Catal.*, 2001, **343**, 5.
24 Gaussian 09, Revision D.01, M. J. Frisch, G. W. Trucks, H. B. Schlegel, G. E. Scuseria, M. A. Robb, J. R. Cheeseman, G. Scalmani, V. Barone, B. Mennucci, G. A. Petersson, H. Nakatsuji, M. Caricato, X. Li, H. P. Hratchian, A. F. Izmaylov, J. Bloino, G. Zheng, J. L. Sonnenberg, M. Hada, M. Ehara, K. Toyota, R. Fukuda, J. Hasegawa, M. Ishida, T. Nakajima, Y. Honda, O. Kitao, H. Nakai, T. Vreven, J. A. Montgomery, Jr., J. E. Peralta, F. Ogliaro, M. Bearpark, J. J. Heyd, E. Brothers, K. N. Kudin, V. N. Staroverov, R. Kobayashi, J. Normand, K. Raghavachari, A. Rendell, J. C. Burant, S. S. Iyengar, J. Tomasi, M. Cossi, N. Rega, J. M. Millam, M. Klene, J. E. Knox, J. B. Cross, V. Bakken, C. Adamo, J. Jaramillo, R. Gomperts, R. E. Stratmann, O. Yazyev, A. J. Austin, R. Cammi, C. Pomelli, J. W. Ochterski, R. L. Martin, K. Morokuma, V. G. Zakrzewski, G. A. Voth, P. Salvador, J. J. Dannenberg, S. Dapprich, A. D. Daniels, Ö. Farkas, J. B. Foresman, J. V. Ortiz, J. Cioslowski, and D. J. Fox, Gaussian, Inc., Wallingford CT, 2009.
25 A. J. Kirby, M. Medeiros, J. R. Mora, P. S. M. Oliveira, A. Amer, N. H. Williams and F. Nome, *J. Org. Chem.*, 2013, **78**, 1343.
26 W. W. Cleland and A. C. Hengge, *Chem. Rev.*, 2006, **106**, 3252.
27 D. M. Brown and D. A. Usher, *J. Chem. Soc.*, 1965, 6558.
28 L. Alderighi, P. Gans, A. Ienco, D. Peters, A. Sabatini and A. Vacca, *Coord. Chem. Rev.*, 1999, **184**, 311.

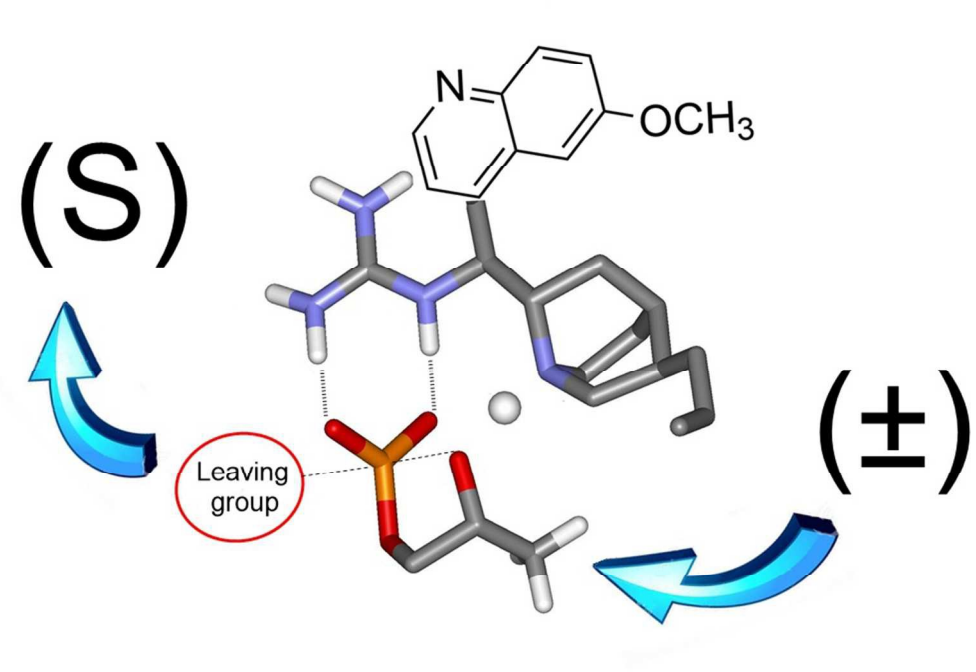

266x189mm (96 x 96 DPI)